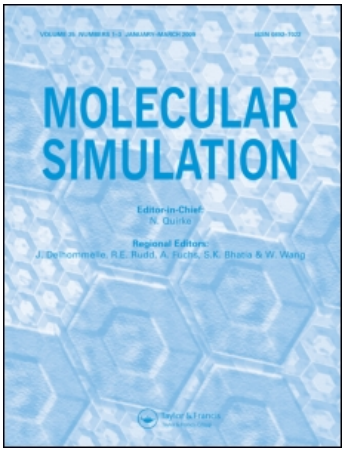

Molecular Simulation
Publication details, including instructions for authors and subscription information:
http://www.informaworld.com/smpp/title~content=t713644482

Multibaric-multithermal molecular dynamics simulation: generalized Nosé-Poincaré-Andersen method

Hisashi Okumura[a]; Yuko Okamoto[a]
[a] Department of Physics, School of Science, Nagoya University, Nagoya, Aichi, Japan

To cite this Article Okumura, Hisashi and Okamoto, Yuko(2007) 'Multibaric-multithermal molecular dynamics simulation: generalized Nosé-Poincaré-Andersen method', Molecular Simulation, 33: 1, 91 — 96
To link to this Article: DOI: 10.1080/08927020601067599
URL: http://dx.doi.org/10.1080/08927020601067599

Molecular Simulation, Vol. 33, Nos. 1–2, 15 January–15 February 2007, 91–96

Taylor & Francis
Taylor & Francis Group

Multibaric–multithermal molecular dynamics simulation: generalized Nosé–Poincaré–Andersen method

HISASHI OKUMURA* and YUKO OKAMOTO†

Department of Physics, School of Science, Nagoya University, Nagoya, Aichi 464-8602, Japan

(Received October 2006; in final form October 2006)

The multibaric–multithermal (MUBATH) algorithm is a generalized-ensemble algorithm with which a random walk both in potential-energy space and in volume space is realized. The MUBATH simulation thus can escape from any local-minimum free-energy states and one can obtain thermodynamic quantities as functions of any temperature and pressure from a single simulation run. We applied the MUBATH molecular dynamics (MD) algorithm to an alanine dipeptide in explicit water. The MUBATH algorithm sampled a wide range of the dihedral-angle space and enabled the simulation to investigate peptide structures including those which cannot be sampled by the conventional isobaric–isothermal simulation.

Keywords: Molecular dynamics simulation; Multibaric–multithermal algorithm; Symplectic integrator; Alanine dipeptide

1. Introduction

Peptides and proteins have complicated free energy surfaces with many local minima. Conventional molecular dynamics (MD) and Monte Carlo (MC) simulations in the canonical or isobaric–isothermal ensemble tend to get trapped in these local minima and can sample only a limited range of configurational space (giving wrong results). In order to avoid this difficulty, generalized-ensemble simulations are commonly performed (for recent reviews, see Ref. [1]). One of the most well-known generalized-ensemble algorithms is the multicanonical algorithm [2–5]. In the multicanonical ensemble, a non-Boltzmann weight factor is used so that a free one-dimensional random walk in the potential-energy space may be realized. Thus, a simulation with this algorithm does not get trapped in free-energy-minimum states and is able to sample a wide range of the configurational space. It is also possible to obtain various canonical-ensemble averages in a wide range of temperature T from a single simulation run by the reweighting techniques [6]. However, the simulation is performed in a fixed volume and we cannot specify pressure as in experimental environment.

In order to overcome this difficulty, we recently proposed the multibaric–multithermal (MUBATH) MC [7–9] and MD [10,11] methods. This is an extension of the multicanonical simulation to realize two-dimensional random walks not only in the potential-energy space but also in the volume space. The MUBATH algorithm has the following advantages: (1) It allows the simulation to escape from any local-minimum-energy state and to sample the configurational space more widely than the conventional isobaric–isothermal method. (2) One can obtain various isobaric–isothermal ensembles not only at any temperature as in the multicanonical algorithm, but also at any pressure from only one simulation run. (3) One can control pressures and temperatures so that we can compare the simulation results with those by experiments under the same condition.

The MUBATH algorithm has been utilized to calculate the equation of states for a super critical fluid [7,8,10,11] and to investigate the liquid–gas phase transition of a Lennard–Jones fluid [9]. In this article, we apply the MUBATH MD method to an alanine dipeptide in explicit water. This is the first work to apply the MUBATH MD algorithm to a biomolecular system.

In Section 2, the algorithm of the MUBATH MD method is explained. Computational details of our MD simulations are described in Section 3. Results and discussion are presented in Section 4. Section 5 is devoted to conclusions.

*Corresponding author. Email: hokumura@tb.phys.nagoya-u.ac.jp
†Email: okamoto@phys.nagoya-u.ac.jp

Molecular Simulation
ISSN 0892-7022 print/ISSN 1029-0435 online © 2007 Taylor & Francis
http://www.tandf.co.uk/journals
DOI: 10.1080/08927020601067599

2. Methods

In the isobaric–isothermal ensemble [12], the distribution $P_{NPT}(E, V)$ for potential energy E and volume V is given by

$$P_{NPT}(E, V) = n(E, V)\, \mathrm{e}^{-\beta_0 H}, \tag{1}$$

where $n(E, V)$ is the density of states as a function of E and V, β_0 is the inverse of the product of the Boltzmann constant k_B and absolute temperature T_0 at which simulations are performed and H is the "enthalpy" (without the kinetic energy contributions):

$$H = E + P_0 V. \tag{2}$$

Here, P_0 is the pressure at which simulations are performed. This ensemble has bell-shaped distributions both in the potential-energy space and in the volume space.

In the MUBATH ensemble [7–11], every state is sampled with a weight factor

$$W_\mathrm{mbt}(E, V) \equiv \exp\{ -\beta_0 H_\mathrm{mbt}(E, V)\} \tag{3}$$

so that a uniform distribution for both E and V may be obtained:

$$P_\mathrm{mbt}(E, V) = n(E, V) W_\mathrm{mbt}(E, V) = \text{constant}. \tag{4}$$

Here, $W_\mathrm{mbt}(E, V)$ and H_mbt are referred to as the MUBATH weight factor and the MUBATH enthalpy, respectively. The difference between H_mbt and H is written as $\delta H(E, V)$:

$$H_\mathrm{mbt}(E, V) = H + \delta H(E, V). \tag{5}$$

The difference $\delta H(E, V)$ is characteristic of the MUBATH simulation.

In this article, the AMBER parm96 force field [13] was used for the peptide and a rigid-body model of the TIP3P force field [14] was used for water molecules. Let the number of atoms in the flexible peptide molecule be N and that of the rigid-body water molecules be M. Atoms in the flexible model molecule are treated in the same way as monatomic molecules in the MD simulations. The Hamiltonian $\mathcal{H}_\mathrm{mbt}$ for the present system is given by the combination of the MUBATH Hamiltonian [10,11] with the Hamiltonian for rigid-body molecules in the isobaric–isothermal ensemble [15]. The isobaric–isothermal Hamiltonian is based on the Nosé thermostat [16,17] and the Andersen barostat [12] with the rigid-body-molecule Hamiltonian [18]:

$$\begin{aligned}\mathcal{H}_\mathrm{mbt} = &\sum_{i=1}^{N+M} \frac{\tilde{\mathbf{p}}_i^2}{2m_i V^{2/3} s^2} \\ &+ \sum_{j=1}^{M} \frac{1}{8s^2} \tilde{\boldsymbol{\pi}}_j^\mathrm{T} \mathbf{S}(\mathbf{q}_j) \mathbf{D}_j \mathbf{S}^\mathrm{T}(\mathbf{q}_j) \tilde{\boldsymbol{\pi}}_j \\ &+ E(V^{1/3}\tilde{\mathbf{r}}, \mathbf{q}) + \frac{P_V^2}{2W} + P_0 V + \frac{P_s^2}{2Q} \\ &+ g k_\mathrm{B} T_0 \log s + \delta H(E(V^{1/3}\tilde{\mathbf{r}}, \mathbf{q}), V),\end{aligned} \tag{6}$$

where the subscript i takes both of the N atoms and the M rigid-body molecules and j takes only M rigid-body molecules. The variable $\tilde{\mathbf{r}}_i$ is the scaled coordinates by the length of the simulation box: $\tilde{\mathbf{r}}_i = V^{-1/3}\mathbf{r}_i$ ($\mathbf{r}_i$ is the real coordinate). We have introduced a simplified notation for the set of the scaled coordinates: $\tilde{\mathbf{r}} \equiv \{\tilde{\mathbf{r}}_1, \tilde{\mathbf{r}}_2, \ldots, \tilde{\mathbf{r}}_{N+M}\}$. When i indicates a rigid-body molecule, $\mathbf{r}_i$ stands for the coordinate of its center of mass. The variable $\tilde{\mathbf{p}}_i$ is the conjugate momentum for $\tilde{\mathbf{r}}_i$. The real momentum $\mathbf{p}_i$ is related to the virtual momentum $\tilde{\mathbf{p}}_i$ by $\mathbf{p}_i = \tilde{\mathbf{p}}_i / V^{1/3} s$, where s is the additional degree of freedom for the Nosé thermostat. The variables P_V and P_s are the conjugate momenta for V and that for s, respectively. The constant m_i is the mass of atom i or rigid-body molecule i. The constants W and Q are the artificial "mass" related to V and s, respectively. The real time interval Δt is associated with the virtual time interval $\Delta \tilde{t}$ by the relation $\Delta t = \Delta \tilde{t}/s$. In the case of the system consisting of N atoms and M rigid-body molecules, g equals $3N + 6M$ if the time development is performed in the real time t, or g equals $3N + 6M + 1$ if the time development is performed in the virtual time $\tilde{t}$. The variable $\mathbf{q}$ is a quaternion which indicates the orientation of the rigid-body molecule. The element of the matrix $\mathbf{S}(\mathbf{q})$ is given by

$$\mathbf{S}(\mathbf{q}) = \begin{pmatrix} q_0 & -q_1 & -q_2 & -q_3 \\ q_1 & q_0 & -q_3 & q_2 \\ q_2 & q_3 & q_0 & -q_1 \\ q_3 & -q_2 & q_1 & q_0 \end{pmatrix}. \tag{7}$$

The variable $\tilde{\boldsymbol{\pi}}_j$ is the conjugate momentum for $\mathbf{q}_j$. The real momentum of the quaternion $\boldsymbol{\pi}_j$ is related to $\tilde{\boldsymbol{\pi}}_j$ by $\boldsymbol{\pi}_j = \tilde{\boldsymbol{\pi}}_j / s$. The matrix $\mathbf{D}$ is a 4×4 matrix consisting of the inverse of the principal moments of inertia I_1, I_2 and I_3:

$$\mathbf{D} = \begin{pmatrix} 0 & 0 & 0 & 0 \\ 0 & I_1^{-1} & 0 & 0 \\ 0 & 0 & I_2^{-1} & 0 \\ 0 & 0 & 0 & I_3^{-1} \end{pmatrix}. \tag{8}$$

The equations of motion are obtained from the Hamiltonian in equation (6). In order to write the equations of motion more elegantly, we may introduce

the angular velocity

$$\boldsymbol{\omega} = (\omega_1, \omega_2, \omega_3)^{\mathrm{T}} \tag{9}$$

and the four-dimensional angular velocity

$$\boldsymbol{\omega}^{(4)} = (0, \omega_1, \omega_2, \omega_3)^{\mathrm{T}}, \tag{10}$$

where ω_1, ω_2, and ω_3 are the angular velocity along each of the corresponding principal axes. The equations of motion in the real time development are then given by

$$\dot{\mathbf{r}}_i = \frac{\mathbf{p}_i}{m_i} + \frac{\dot{V}}{3V}\mathbf{r}_i, \tag{11}$$

$$\dot{\mathbf{p}}_i = \left(1 + \frac{\partial \delta H}{\partial E}\right)\mathbf{F}_i - \left(\frac{\dot{V}}{3V} + \frac{\dot{s}}{s}\right)\mathbf{p}_i, \tag{12}$$

$$\dot{\mathbf{q}}_j = \frac{1}{2}\mathbf{S}(\mathbf{q}_j)\omega_j^{(4)}, \tag{13}$$

$$\mathbf{I}_j\dot{\omega}_j = \left(1 + \frac{\partial \delta H}{\partial E}\right)\mathbf{N}_j - \omega_j \times (\mathbf{I}_j\omega_j) - \frac{\dot{s}}{s}I_j\omega_j, \tag{14}$$

$$\dot{V} = s\frac{P_V}{W}, \tag{15}$$

$$\dot{P}_V = s\left[\frac{1}{3V}\left\{\sum_{i=1}^{N+M}\frac{p_i^2}{m_i} + \left(1 + \frac{\partial \delta H}{\partial E}\right)\sum_{i=1}^{N+M}\mathbf{F}_i\cdot\mathbf{r}_i\right\} - \left(P_0 + \frac{\partial \delta H}{\partial V}\right)\right], \tag{16}$$

$$\dot{s} = s\frac{P_s}{Q}, \tag{17}$$

$$\dot{P}_s = \sum_{i=1}^{N+M}\frac{\mathbf{p}_i^2}{m_i} + \sum_{j=1}^{M}\omega_j^{\mathrm{T}}\mathbf{I}_j\omega_j - gk_{\mathrm{B}}T_0, \tag{18}$$

where $\mathbf{I}$ is the 3×3 diagonal matrix whose diagonal elements are I_1, I_2 and I_3. The vector $\mathbf{F}_i$ stands for the force acting on the atom i if i indicates an atom in the flexible molecule or the total force on all the atoms in molecule i if i indicates a rigid-body molecule. The vector $\mathbf{N}_j$ is the torque of molecule j. Performing the MD simulation by these equations of motion in equations (11)–(18), the MUBATH distribution $P_{\mathrm{mbt}}(E, V)$ in equation (4) is realized.

For the actual time development in equations (11)–(18), a symplectic integrator was employed in the present simulations. We used the symplectic time-development formalism [15] which is based on the Nosé–Poincaré thermostat [19,20], the Andersen barostat [12] and the symplectic quaternion scheme [18]. The Nosé–Poincaré thermostat gives the same equations of motion as the Nosé thermostat and provides a symplectic integrator. Combining these three algorithms, we perform the time development by the symplectic integrator throughout the simulation. The symplectic integrator has the advantage that the secular deviation of the value of the Hamiltonian is suppressed.

In the case of

$$\delta H(E, V) = \frac{\partial \delta H(E, V)}{\partial E} = \frac{\partial \delta H(E, V)}{\partial V} = 0, \tag{19}$$

the Hamiltonian in equation (6) and the equations of motion in equations (11)–(18) become those for the isobaric–isothermal MD simulation of the Nosé–Andersen formulation for the system consisting of both flexible and rigid-body molecules. The MUBATH weight factor is, however, not *a priori* known and has to be determined by the usual iterations of short simulations [21,22].

After an optimal weight factor $W_{\mathrm{mbt}}(E, V)$ is determined, a long production run is performed for data collection. We use the reweighting techniques [6] for the results of the production run to calculate the isobaric–isothermal-ensemble averages. The probability distribution $P_{NPT}(E, V; T, P)$ in the isobaric–isothermal ensemble at the desired temperature T and pressure P is given by

$$P_{NPT}(E,V;T,P) = \frac{P_{\mathrm{mbt}}(E,V)W_{\mathrm{mbt}}^{-1}(E,V)\mathrm{e}^{-\beta(E+PV)}}{\int \mathrm{d}V \int \mathrm{d}E P_{\mathrm{mbt}}(E,V)W_{\mathrm{mbt}}^{-1}(E,V)\mathrm{e}^{-\beta(E+PV)}}. \tag{20}$$

The expectation value of a physical quantity A at T and P is then obtained from

$$\langle A\rangle_{NPT} = \int \mathrm{d}V \int \mathrm{d}E\, A(E,V)P_{NPT}(E,V;T,P) \tag{21}$$

$$= \frac{\langle A(E,V)W_{\mathrm{mbt}}^{-1}(E,V)\mathrm{e}^{-\beta(E+PV)}\rangle_{\mathrm{mbt}}}{\langle W_{\mathrm{mbt}}^{-1}(E,V)\mathrm{e}^{-\beta(E+PV)}\rangle_{\mathrm{mbt}}}, \tag{22}$$

where $\langle\cdots\rangle_{\mathrm{mbt}}$ is the MUBATH ensemble average. Because of the random walks both in the potential-energy space and in the volume space, we can calculate physical quantities in wide ranges of T and P.

3. Computational details

The MUBATH MD simulation was performed for a system consisting of one alanine dipeptide molecule (*N*-acetyl-alanine-*N*′-methylamide) and 63 water molecules. We used the AMBER parm96 force field [13] for the alanine dipeptide molecule and the TIP3P [14] rigid-body model for the water molecules. The initial values of the alanine dipeptide dihedral-angles were $\phi = \psi = 180°$ as shown in figure 1. We employed a cubic unit cell with

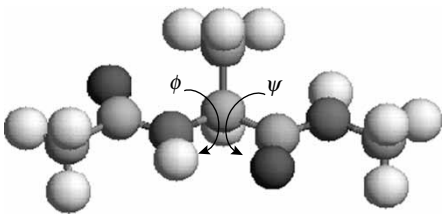

Figure 1. The initial condition of alanine dipeptide. Its dihedral angles are $\phi = \psi = 180°$.

periodic boundary conditions. The electrostatic potential was calculated by the Ewald method. We calculated the van der Waals interaction, which is given by the Lennerd–Jones term, of all pairs of the molecules within the minimum image convention instead of introducing the spherical potential cutoff. The time step was taken as $\Delta t = 0.5$ fs.

In order to obtain an optimal MUBATH weight factor $W_{\mathrm{mbt}}(E, V)$, a two-dimensional version [9] of the energy landscape paving method [23] for multicanonical weight factor determination was employed. This is a special case of the Wang–Landau techniques [24]. This technique updates $W_{\mathrm{mbt}}(E, V)$ at every MD step t as $W_{\mathrm{mbt}}(E, V, t) \equiv \exp\{ - H_{\mathrm{mbt}}(E, V, t)/k_{\mathrm{B}}T_0\}$ to lower energy barriers. We obtained an optimal weight factor $W_{\mathrm{mbt}}(E, V)$ after this preliminary simulation for 2.61 ns. We then performed a long MUBATH MD simulation for data collection for 10 ns after an equilibration process for 10 ps.

For convenience, we discretized E and V into bins and used histograms to calculate $\delta H(E, V)$. We chose the bin sizes of $\Delta E = 20$ kcal/mol and $\Delta V = 0.1$ nm^3. In order to calculate the derivative of $\delta H(E, V)$ such as $\partial \delta H(E, V)/\partial E$ and $\partial \delta H(E, V)/\partial V$, it is necessary to interpolate the histogram. We interpolated the histogram by the third-order polynomial in both E and V to make these derivatives continuous at the boundaries between two adjacent bins (see Ref. [11]). Deviation of the value of the Hamiltonian from its initial value is suppressed by this polynomial.

In order to compare the MUBATH simulation with the conventional isobaric–isothermal one, we also performed the isobaric–isothermal MD simulations of the same system, which consists of an alanine dipeptide molecule in 63 water molecules. The simulation was carried out at $T_0 = 250$ K and $P_0 = 0.1$ MPa for 1 ns.

4. Results and discussion

We now present the results of our MD simulations. The time series of potential energy E from the conventional isobaric–isothermal MD simulation at $T_0 = 250$ K and $P_0 = 0.1$ MPa is shown in figure 2(a). The potential energy fluctuates in a narrow range of $E = -710 \sim -630$ kcal/mol. On the other hand, figure 2(b) shows that the MUBATH MD simulation realizes a random walk in the potential-energy space and covers a wide energy range. The covered range is $E = -730 \sim -280$ kcal/mol and 5.8 times wider than that by the isobaric–isothermal MD.

Figure 3(a) shows the time series of volume V obtained by the conventional isobaric–isothermal MD simulations. The volume fluctuates only in a range of $V = 1.9 \sim 2.4$ nm^3. The MUBATH MD simulation, on the other hand, performs a random walk that covers a range of $V = 1.8 \sim 3.5$ nm^3, as shown in figure 3(b), which is 3.6 times wider than that by the isobaric–isothermal MD.

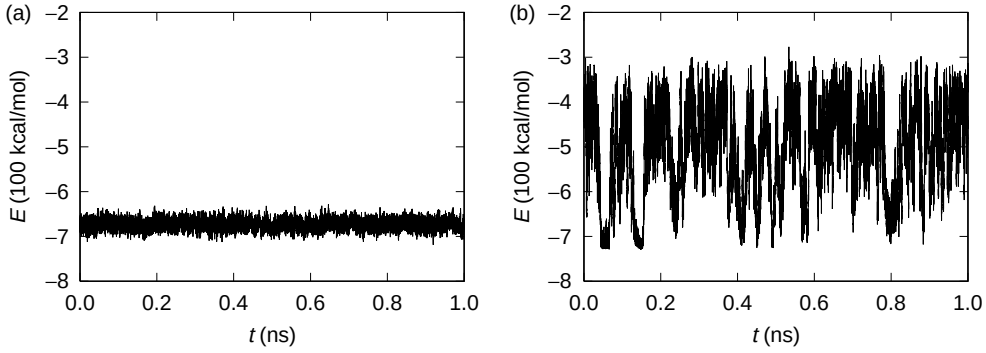

Figure 2. The time series of potential energy E from (a) the conventional isobaric–isothermal MD simulation at $T_0 = 250$ K and $P_0 = 0.1$ MPa and (b) the MUBATH MD simulation.

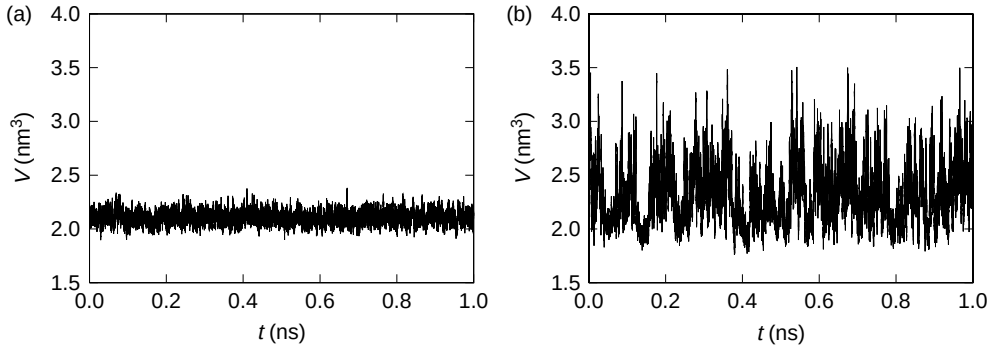

Figure 3. The time series of volume V from (a) the conventional isobaric–isothermal MD simulation and (b) the MUBATH MD simulation.

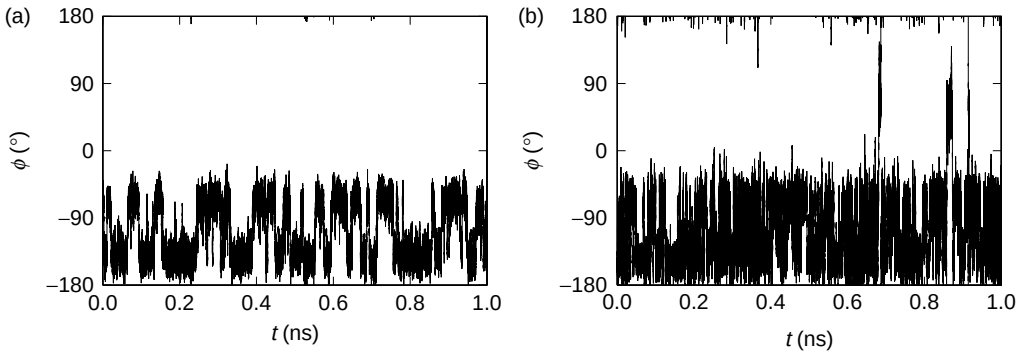

Figure 4. The time series of the backbone dihedral angle ϕ from (a) the conventional isobaric–isothermal MD simulation and (b) the MUBATH MD simulation.

The time series of the dihedral angle ϕ in the isobaric–isothermal MD is given in figure 4(a). The dihedral angle ϕ rotates less than half a rotation (covering less than a 180° range). This fact shows that it is trapped in local-minimum free-energy states and does not rotate beyond the energy barriers. In the MUBATH MD simulation, on the other hand, ϕ goes through entire rotation (covering 360°) three times in the time range of 1 ns as shown in figure 4(b). It rotates 24 times throughout the simulation of 10 ns (It is not shown).

We show the time series of the dihedral angle ψ in figure 5. Similarly to the case of ϕ, the isobaric–isothermal MD simulation tends to be trapped in local-minimum free-energy states. The dihedral angle ψ rotates only once during 1 ns, as shown in figure 5(a). The efficiency of the MUBATH MD for ψ is also remarkable as for ϕ. The dihedral angel ψ experiences entire rotations 24 times during 1 ns, as shown in figure 5(b). It rotates 242 times throughout the simulation of 10 ns. The wide rotation ranges of ϕ and ψ show that the simulation in the MUBATH ensemble can escape from local-minimum free-energy states and samples the configurational space much more widely than the conventional isobaric–isothermal ensemble.

The probability distributions $P(\phi, \psi)$ of ϕ and ψ at $T = 250\,\mathrm{K}$ and $P = 0.1\,\mathrm{MPa}$ are shown in figure 6. Figure 6(a) shows that $P(\phi, \psi)$ obtained by the isobaric–isothermal MD simulation has only three peaks: P_{II}, C_5, and α_{P}. No other state was sampled by the isobaric–isothermal MD simulation. It means that the isobaric–isothermal MD is trapped in the local minima. Figure 6(b) shows $P(\phi, \psi)$ obtained by the reweighting procedure at $T = 250\,\mathrm{K}$ and $P = 0.1\,\mathrm{MPa}$ from the MUBATH MD simulation. The MUBATH MD simulation samples not only the states of P_{II}, C_5, and α_{P} but also α_{R} and α_{L}. These results indicate again that the MUBATH simulation can get over the free energy barriers and has a high sampling efficiency. Peak position of $P(\phi, \psi)$ for each state is shown in table 1.

5. Conclusions

We applied the MUBATH MD method to alanine dipeptide in explicit water. This method has an advantage that the simulation performs a two-dimensional random walk both in the potential-energy space and in the volume space so that it allows the simulation to escape from local-minimum free-energy states. It sampled the states of P_{II}, C_5, α_{P}, α_{R}, and α_{L}. On the other hand, the conventional isobaric–isothermal simulation was trapped in local-minimum free-energy states and sampled not all of them.

The other advantages of the MUBATH MD method are that one can control temperature and pressure similarly to real experimental conditions and obtain various isobaric–isothermal ensemble averages from only one simulation

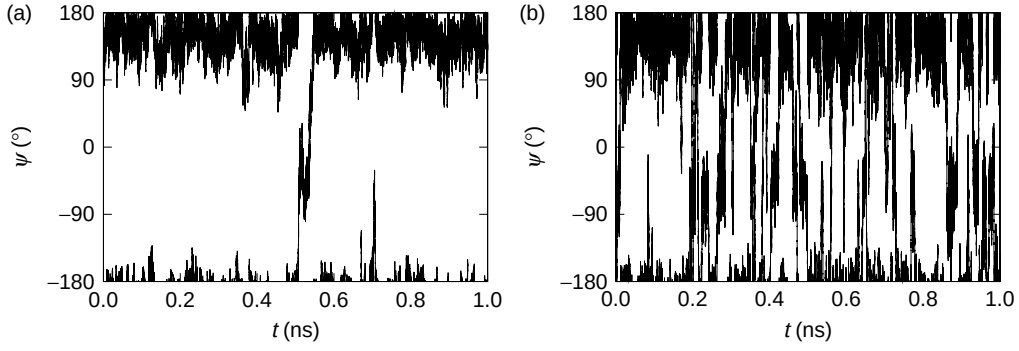

Figure 5. The time series of the backbone dihedral angle ψ from (a) the conventional isobaric–isothermal MD simulation and (b) the MUBATH MD simulation.

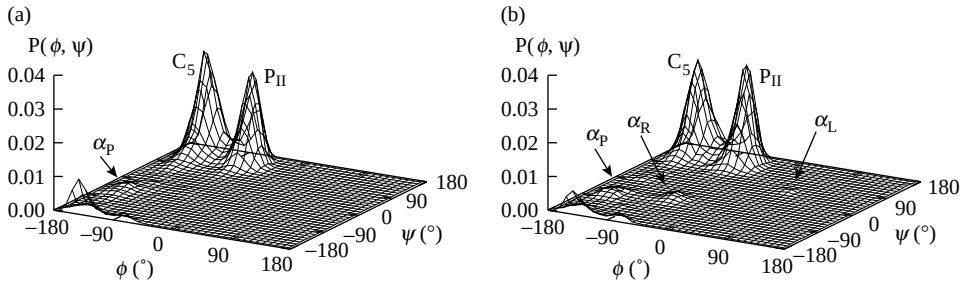

Figure 6. The probability distributions $P(\phi, \psi)$ of the backbone dihedral angles ϕ and ψ at $T = 250\,\mathrm{K}$ and $P = 0.1\,\mathrm{MPa}$ from (a) the conventional isobaric–isothermal MD simulation and (b) the MUBATH MD simulation by the reweighting techniques.

Table 1. Peak position (ϕ, ψ) of the probability distribution $P(\phi,\psi)$ for each state, which is obtained by the reweighting procedure at $T = 250\,\mathrm{K}$ and $P = 0.1\,\mathrm{MPa}$ from the MUBATH MD simulation.

	ϕ	ψ
P_{II}	$-65°$	$145°$
C_5	$-145°$	$155°$
α_R	$-65°$	$-45°$
α_L	$55°$	$55°$
α_P	$-155°$	$-75°$

run. In order to study the temperature and pressure dependences of the protein structures, one has to investigate its free energy surface at several values of temperature and pressure. The MUBATH method will thus be of great use for the protein folding problem under various conditions of temperature and pressure.

Acknowledgements

This work was supported, in part, by the Grants-in-Aid for the Next Generation Super Computing Project, Nanoscience Program and for Scientific Research in Priority Areas, "Water and Biomolecules", from the Ministry of Education, Culture, Sports, Science and Technology, Japan.

References

[1] A. Mitsutake, Y. Sugita, Y. Okamoto. Generalized-ensemble algorithms for molecular simulations of biopolymers. *Biopolym. Pept. Sci.*, **60**, 96 (2001).
[2] B.A. Berg, T. Neuhaus. Multicanonical algorithms for first-order phase transitions. *Phys. Lett. B*, **267**, 249 (1991).
[3] B.A. Berg, T. Neuhaus. Multicanonical ensemble: a new approach to simulate first-order phase transitions. *Phys. Rev. Lett.*, **68**, 9 (1992).
[4] U.H.E. Hansmann, Y. Okamoto, F. Eisenmenger. Molecular dynamics, Langevin and hybrid Monte Carlo simulations in a multicanonical ensemble. *Chem. Phys. Lett.*, **259**, 321 (1996).
[5] N. Nakajima, H. Nakamura, A. Kidera. Multicanonical ensemble generated by molecular dynamics simulation for enhanced conformational sampling of peptides. *J. Phys. Chem. B*, **101**, 817 (1997).
[6] A.M. Ferrenberg, R.H. Swendsen. New Monte Carlo technique for studying phase transitions. *Phys. Rev. Lett.*, **61**, 2635 (1988); *ibid.*, **63**, (1989) 1658(E).
[7] H. Okumura, Y. Okamoto. Monte Carlo simulations in multibaric–multithermal ensemble. *Chem. Phys. Lett.*, **383**, 391 (2004).
[8] H. Okumura, Y. Okamoto. Monte Carlo simulations in generalized isobaric–isothermal ensembles. *Phys. Rev. E*, **70**, 026702 (2004).
[9] H. Okumura, Y. Okamoto. Liquid–gas transition by the multibaric–multithermal simulation. *J. Phys. Soc. Jpn.*, **73**, 3304 (2004).
[10] H. Okumura, Y. Okamoto. Molecular dynamics simulation in the multibaric–multithermal ensemble. *Chem. Phys. Lett.*, **391**, 248 (2004).
[11] H. Okumura, Y. Okamoto. Multibaric–multithermal ensemble molecular dynamics simulations. *J. Comput. Chem.*, **27**, 379 (2006).
[12] H.C. Andersen. Molecular dynamics simulations at constant pressure and/or temperature. *J. Chem. Phys.*, **72**, 2384 (1980).
[13] P.A. Kollman, R. Dixon, W. Cornell, T. Fox, C. Chipot, A. Pohorille. In *Computer Simulation of Biomolecular Systems*, A. Wilkinson, P. Weiner, W.F. van Gunsteren (Eds.), p. 83, Elsevier (1997).
[14] W.L. Jorgensen, J. Chandrasekhar, J.D. Madura, R.W. Impey, M.L. Klein. Comparison of simple potential functions for simulating liquid water. *J. Chem. Phys.*, **79**, 926 (1983).
[15] H. Okumura, S.G. Itoh, Y. Okamoto. Explicit symplectic integrators of molecular dynamics algorithms for rigid-body molecules in the canonical, isothermal–isobaric, and related ensembles. *J. Chem. Phys.*, submitted. (2006).
[16] S. Nosé. A molecular dynamics method for simulations in the canonical ensemble. *Mol. Phys.*, **52**, 255 (1984).
[17] S. Nosé. A unified formation of the constant temperature molecular dynamics methods. *J. Chem. Phys.*, **81**, 511 (1984).
[18] T.F. Miller, M. Eleftheriou, P. Pattnaik, A. Ndirango, D. Newns, G.J. Martyna. Symplectic quaternion scheme for biophysical molecular dynamics. *J. Chem. Phys.*, **116**, 8649 (2002).
[19] S.D. Bond, B.J. Leimkuhler, B.B. Laird. The Nosé–Poincaré method for constant temperature molecular dynamics. *J. Comput. Phys.*, **151**, 114 (1999).
[20] S. Nosé. An improved symplectic integrator for Nosé–Poincaré thermostat. *J. Phys. Soc. Jpn.*, **70**, 75 (2001).
[21] B.A. Berg, T. Celik. New approach to spin-glass simulations. *Phys. Rev. Lett.*, **99**, 2292 (1992).
[22] Y. Okamoto, U.H.E. Hansmann. Thermodynamics of helix-coil transitions studied by multicanonical algorithms. *J. Phys. Chem.*, **99**, 11276 (1995).
[23] U.H.E. Hansmann, L.T. Wille. Global optimization by energy landscape paving. *Phys. Rev. Lett.*, **88**, 068105 (2002).
[24] F. Wang, D.P. Landau. Efficient, multiple-range random walk algorithm to calculate the density of states. *Phys. Rev. Lett.*, **86**, 2050 (2001).